Application of fluorescent Eu:Gd_2O_3 nanoparticles to the visualization of protein micropatterns

Dosi Dosev[a], Mikaela Nichkova[b], Maozi Liu[c], Bing Guo[a],
Gang-yu Liu[c], Younan Xia[d], Bruce D. Hammock[b], Ian M. Kennedy[a*]

[a] Department of Mechanical and Aeronautical Engineering, [b] Department of Entomology,
[c] Department of Chemistry University of California Davis, Davis CA, USA 95616
[d] Department of Chemistry, University of Washington, Seattle, Washington, 98195

ABSTRACT

Nanoparticles made of lanthanide oxides are promising fluorophores as a new class of tags in biochemistry because of their large Stokes shift, sharp emission spectra, long lifetime and lack of photobleaching. We demonstrate for first time the application of these nanoparticles to the visualization of protein micropatterns. Europium-doped gadolinium oxide (Eu:Gd_2O_3) nanoparticles were synthesized by spray pyrolysis and were characterized by means of laser-induced fluorescent spectroscopy and TEM. Their main emission peak is at 612 nm. And their size distribution is from 5 nm to 500 nm. The nanoparticles were coated with avidin through physical adsorption. Biotinylated Bovine Serum Albumin (BSA-b) was patterned on a silicon wafer using a micro-contact printing technique. The BSA-b - patterned wafer was incubated in a solution containing the avidin-coated nanoparticles. The specific interaction between biotin and avidin was studied by means of fluorescent microscopy and atomic-force microscopy (AFM). The fluorescent microscopic images revealed that the nanoparticles were organized into designated structures as defined by the microcontact printing process – non-specific binding of the avidin-coated nanoparticles to bare substrate was negligible. The fluorescent pattern did not suffer any photobleaching during the observation process which demonstrates the suitability of Eu:Gd_2O_3 nanoparticles as fluorescent labels with extended excitation periods – organic dyes, including chelates, suffer bleaching over the same period. More detailed studies were preformed using AFM at a single nanoparticle level. The specific and the non-specific binding densities of the particles were qualitatively evaluated.

Keywords: nanoparticles, lanthanide, fluorescence, biosensor, microcontact printing, AFM

1. INTRODUCTION

Fluorescent nanoparticles are emerging materials that offer new possibilities in biotechnology. Their main advantage when compared with the conventionally used organic dyes is the enhanced photostability. Lanthanide oxides are commonly used fluorescent materials in the lighting industry[1,2]. Nanoparticles of lanthanide oxides are promising for labels in biotechnology because of their optical properties such as large Stokes shift, lack of photobleaching and long fluorescence lifetime (about 1 ms). The large Stokes shift allows the subtraction of the excitation wavelength by filtering, while the long lifetime allows for time-gated detection and subtraction of the background fluorescence. In addition, the synthesis of lanthanide oxides can be quick, simple and scalable for mass production. Particles with different emission wavelengths can be easily obtained by controlled doping of lanthanide ions into an appropriate host material [3]. In contrast with semiconductor quantum dots [4], the emission wavelength of the lanthanide oxide nanoparticles is independent on the particle size, thus size is not a critical issue for the spectral properties. This allows us to work within a certain size range that is mainly determined by the particular application. The unique properties of the lanthanide oxide nanoparticles make them promising for low-cost applications in biochemistry. First results using Europium oxide (Eu_2O_3) nanoparticles as labels for environmental immunoassay have already been reported showing enhanced assay sensitivity [5].

* imkennedy@ucdavis.edu; phone 1530 7522796; fax 1 530 2108220

Imaging, Manipulation, and Analysis of Biomolecules and Cells: Fundamentals and Applications III,
D. V. Nicolau, J. Enderlein, R. C. Leif, D. L. Farkas, R. Raghavachari, eds., Proc. of SPIE Vol. 5699
(SPIE, Bellingham, WA, 2005) · 1605-7422/05/$15 · doi: 10.1117/12.588722

Emerging techniques in biochemistry and biosensor development are based on protein and DNA microarrays formed by micro contact printing [6]. Microarrays are usually visualized under fluorescent microscopes using organic fluorescent dyes [7]. Dye photobleaching could reduce significantly the available time for observation, thus, photostability of the fluorophores is of crucial importance for this type of applications.

In this work, we demonstrate the use of Europium-doped Gadolinium oxide ($Eu:Gd_2O_3$) nanoparticles as fluorophores for visualization of protein micropatterns. Avidin – biotin specific binding is used as a model system.

2. EXPERIMENTAL

2.1. Chemicals and Materials.

Europium (III) nitrate $Eu(NO_3)_3.5H_2O$ and gadolinium (III) nitrate $Gd(NO_3)_3.6H_2O$ for the synthesis of fluorescent $Eu:Gd_2O_3$ were purchased from Sigma. Avidin and bovine serum albumin (BSA) were obtained from Sigma. ImmunoPure Biotinylated BSA (BSA-b, 8 moles Biotin/mol protein) was purchased from Pierce. 5-carboxyrhodamine 6G, succinimidyl ester was obtained from Sigma. Avidin-Rhodamine 6G was prepared by a conjugation reaction between the amine groups of the protein and the succinimidyl ester of the 5-carboxyrhodamine 6G following a standard procedure recommended by Molecular Probes [8]. The degree of labeling obtained was 2 moles rhodamine/mol avidin. Deionized water (18 MΩ·cm) was obtained using a Millipore purification system. Phosphate buffer saline (PBS) (pH=7.5) was 10 mM phosphate buffer, 0.8% saline. Black 96-well plates from Nunc were used for fluorescence measurements. The polydimethylsiloxane (PDMS) stamp used in micro-contact printing has a line width of 5 μm. The n-doped Si wafer was used as a substrate for micro-contact printing and AFM characterization.

2.2. Instrumentation.

The size and the morphology of the $Eu:Gd_2O_3$ nanoparticles were determined using Philips CM-12 Transmission Electron Microscope (TEM). An Opolette™ tunable pulsed optical parametric oscillator (OPO) laser (Opotek, CA) was used for fluorescence excitation of the nanoparticles and their fluorescence spectra were recorded using a Spectra Pro 300i gated intensified spectrometer (Princeton Instruments Inc). A Spectramax M2 microplate reader (Molecular Dveices, Sunnyvale, CA) was used for the detection of rhodamine fluorescence. An ultrasonic bath 75D (VWR) was used for treating the nanoparticles suspensions and for cleaning procedures. The centrifuges used for nanoparticle sizing were Sorvall® RC5B Plus Centrifuge (Kendro Laboratory Products) and Centrifuge 5415D (Eppendorf). Fluorescent microscope Nicon Microphot-SA equipped with 400 nm Dichroic Mirror Cube DM 400 and 100 W Mercury lamp was used for observation of the fluorescent micropatterns. A computer – controlled CCD camera RT Color, model 2.2.1 from Diagnostic Instruments Inc. was coupled to the fluorescent microscope and was used for digital visualization of the fluorescent images. The atomic force microscopy (AFM) used for this paper is a MFP-3D (Asylum Research, Santa Barbara, CA). The ultrasharpened Si_3N_4 AFM tip was obtained from Veeco (Santa Barbara, CA) with a spring constant of 0.1 nN m^{-1}.

2.3. Synthesis of $Eu:Gd_2O_3$ nanoparticles.

Fluorescent $Eu:Gd_2O_3$ were synthesized by a spray pyrolysis method that is described elsewhere [9]. Briefly, an ethanol solution containing 20 mM $Eu(NO_3)_3$ and 80 mM $Gd(NO_3)_3$ was sprayed into a hydrogen diffusion flame through a neubilizer. The flame was formed by an H_2 flow at 2 L min^{-1} and an air co-flow at 10 L min^{-1}, surrounding the outlet of the nebulizer. A flame temperature above 2100°C was reached. Oxidation reactions took place within the flame to form $Eu:Gd_2O_3$ nanoparticles. A cold finger was used for collecting the $Eu:Gd_2O_3$ particles thermophoretically. The production rate of this synthesis procedure was about 400 – 500 mg h^{-1}. The as-synthesized particles were suspended in methanol in an ultrasonic bath for 30 min in order to break any weak agglomerates formed during the collection process. Particles larger than 200 nm diameter were settled from the primary suspension by means of selective centrifugation at 1000×g for 2 min. The nanoparticles from the supernatant (diameter below 200 nm) were extracted and dried for subsequent use.

2.4. Coating of Eu:Gd_2O_3 nanoparticles with avidin.

Eu:Gd_2O_3 nanoparticles (1 mg) were suspended using ultrasonic bath in 1 ml of 25 mM carbonate-bicarbonate buffer, pH=8.6 in a polypropylene tube, previously coated with 0.5% BSA to avoid loss of avidin to the tube walls. A solution of 2 mg ml^{-1} avidin (100 µl) were added to the particle suspension and incubated in a rotating mill overnight at room temperature. The suspension was then centrifuged at 15000×g for 3 minutes. The supernatant was discarded and the nanoparticle pellet was resuspended in the same buffer for washing off the excess of the protein. This procedure was repeated 3 times. In order to ensure that there was no bare particle surface left, the avidin - Eu:Gd_2O_3 nanoparticles were incubated in 1 ml of 0.5 mg ml^{-1} BSA solution in 25 mM phosphate buffer for 1 h at room temperature in the rotating mill. After three consecutive washings by centrifugation and resuspension, the avidin - Eu:Gd_2O_3 nanoparticles were used for the micropattern detection assays. The surface saturation capacity of the nanoparticles for avidin was evaluated following the same coating procedure but using avidin-rhodamine complex instead of avidin. After efficient washing of the excess avidin-rhodamine from the coating solution, the nanoparticle pellet was resuspended in 100 µl of carbonate-bicarbonate buffer. The fluorescence of rhodamine (excitation 520 nm, emission 550 nm) adsorbed on the particle surface was measured on the microplate reader. Rhodamine fluorescence intensity was used as an indication for the amount of adsorbed avidin molecules.

2.5. Microcontact printing of biotinylated BSA. Substrate, stamp and sample preparation.

A silicon wafer with crystallographic orientation (100) was used as a solid substrate for microcontact printing of proteins and the consecutive specific interactions. Prior to use, the silicon wafer was thoroughly washed in ultrasound bath in acetone, ethanol and deionized water for 10 min each. Finally, it was dried under a blowing nitrogen stream. The PDMS stamp was washed by sonication in ethanol (3x10 min), dried under nitrogen and exposed to the solution of the inking protein (50 µg ml^{-1} BSA-b in PBS) for 40 min. Excess solution was removed, and the stamp was dried under a stream of nitrogen gas. After inking, the stamp was brought into contact with the silicon wafer substrate and a very small amount of force was applied to make a good contact between both surfaces. The stamp was removed after 2 min, and the wafer was rinsed with PBS and deionized water and dried under nitrogen. The stamp could be used about 50 times without degradation of the printing capability when rinsed with water, water:ethanol mixture (80:20) and cleaned by sonication in ethanol (3 x 10 min) after each inking and printing cycle.

The BSA-b printing procedure is schematically presented in Fig. 1a. After micro contact printing of the BSA-b, the

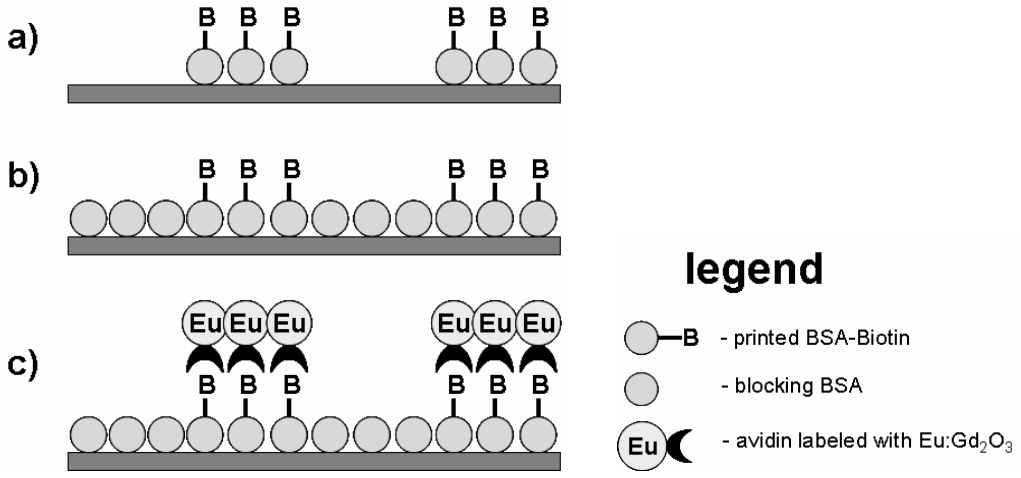

Figure 1. Schematic description of microcontact printing of BSA-biotin **(a)**, blocking with BSA **(b)**, and specific interaction biotin – avidin-Eu:Gd_2O_3 **(c)**.

uncovered areas on the silicon substrate were blocked with 2 mg ml^{-1} of BSA solution in PBS for 1 h (Fig. 1b) in order to avoid further non-specific binding and/or sticking. After washing and drying, the wafer was incubated with a suspension of the avidin coated Eu:Gd_2O_3 nanoparticles in carbonate-bicarbonate buffer) for 1 h in a shaker allowing for specific interaction between the avidin and biotin to occur (Fig. 1c). After the interaction took place the substrate was rinsed with buffer, water and dried under nitrogen before fluorescence and AFM studies.

2.6. Fluorescence microscopy imaging.

Fluorescent images were acquired with fluorescent microscope equipped with computer - controlled CCD camera. A 100 W Hg lamp was used to excite fluorescence of the Eu:Gd_2O_3 nanoparticles. A dichroic cube with a threshold wavelength of 400 nm was used to separate the UV excitation (λ_{ex}<400 nm) from the visible fluorescence emission (λ_{em}>400 nm). The CCD camera was controlled and the images were captured and analyzed using "Spot" software.

2.7. Atom force microscopy characterization

All the AFM images were taken at contact mode with a scan speed of 1-2 Hz. The image force was under 5 nN. The topography and lateral force images were taken in air at room temperature.

3. RESULTS AND DISCUSSION

3.1. Properties of the Eu:Gd_2O_3 nanoparticles

According to TEM analysis [9], most of the primarily obtained particles have sizes between 5 and 500 nm and are nearly spherical shape. A narrower size distribution was obtained by means of selective centrifugation between 5 and 200 nm. Figure 1 represents a typical bright field TEM micrograph of the sized nanoparticles. Three particles with sizes about 100 nm can be observed on the figure and one with diameter of 15 nm. They have a dense morphology and approximately spherical shape although not a perfect sphere as in other synthesis methods.

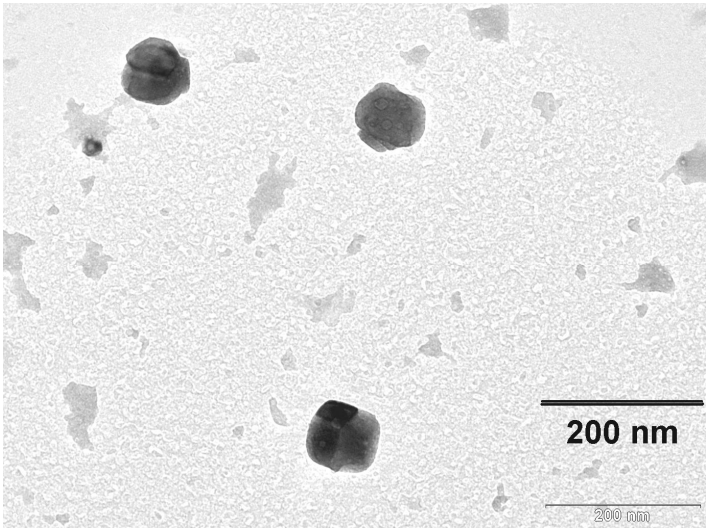

Figure 2. Bright field electron micrograph of Eu:Gd_2O_3 nanoparticles obtained by spray pyrolysis

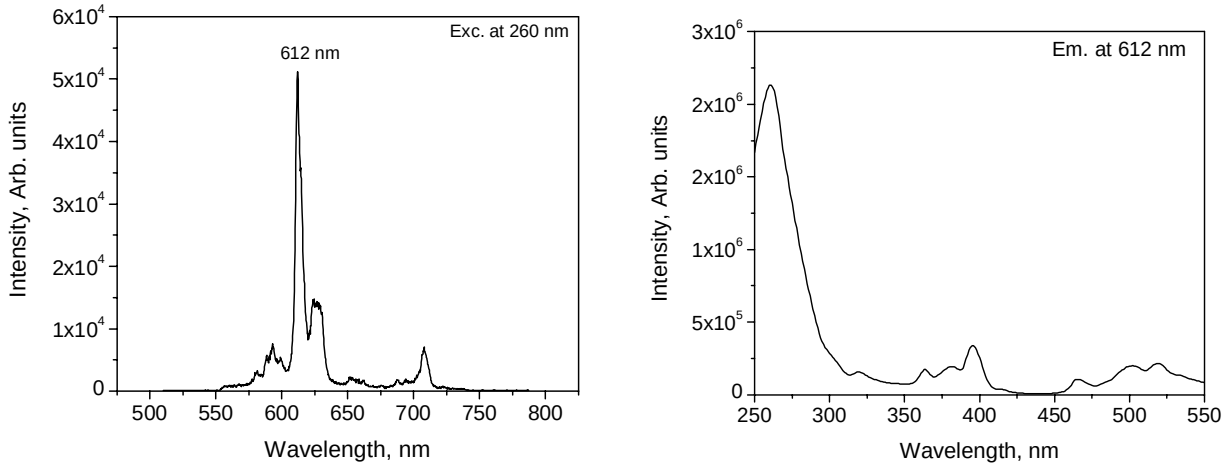

Figure 3. Fluorescence emission (left) and excitation (right) spectra of the Eu:Gd_2O_3 nanoparticles

The fluorescence properties of the Eu:Gd_2O_3 nanoparticles were studied by using laser – induced fluorescence. A colloidal solution of 1 mg ml^{-1} in methanol was excited with a pulsed laser beam at 260 nm wavelength.

The fluorescence emission spectrum from Fig. 3 (left) shows main emission peak at 612 nm, which corresponds to the $^5D_0 \rightarrow {}^7F_2$ transition of the Eu^{3+} ion in the Gd_2O_3 crystal lattice [3]. The half-width of the peak is 5 nm which is very narrow in comparison with other fluorophores. The excitation spectrum from Fig. 3 (right) reveals multiple excitation peaks far from the emission at 612 nm. The most efficient excitation is in the UV range between 250 and 280 nm. Some additional excitation peaks are distributed in the range 350-400 nm and 450-550 respectively. This offers the possibility to choose between different excitation sources according to the experimental setup and the application.

3.2. Coating of the nanoparticles with avidin

Because the avidin-biotin interaction has a high binding constant, this assay is widely used and in molecular biology, immunoassay, diagnostics, and biosensor research. A demonstration using the avidin and biotin reaction system is the logical first step in an evaluation of a new format for biosensors, protein chips, and other miniaturized analytical devices. Thus, we have chosen the avidin-biotin system as a model system in our studies in order to demonstrate the approach of using Eu:Gd_2O_3 nanoparticles as fluorescent labels for micropattern imaging.
Avidin, a highly positively charged protein was found to adsorb tightly to negatively charged surfaces, such as dye-doped silica nanoparticles [10] and quantum dots [11, 12]. Here, we take advantage of the negatively charged surface of the Gd_2O_3 nanoparticles to coat them directly based on the electrostatic interactions with the avidin molecules. The surface of the Eu:Gd_2O_3 nanoparticles was coated with a monolayer of avidin. The coating was carried out by physical adsorption of avidin to the nanoparticle surface according to the above described experimental procedure. There are several advantages offered by this coating method: it is a one step procedure (thereby avoiding chemical functionalization and conjugation steps); proteins retain their activity; conjugates are stable in a variety of buffers; the number of binding sites on the surface can be controlled by varying the coating concentration and can be quantified easily; the nanoparticles' fluorescence is not affected by the protein layer; the nanoparticle surface can be efficiently blocked to avoid non-specific binding in immunoassays.

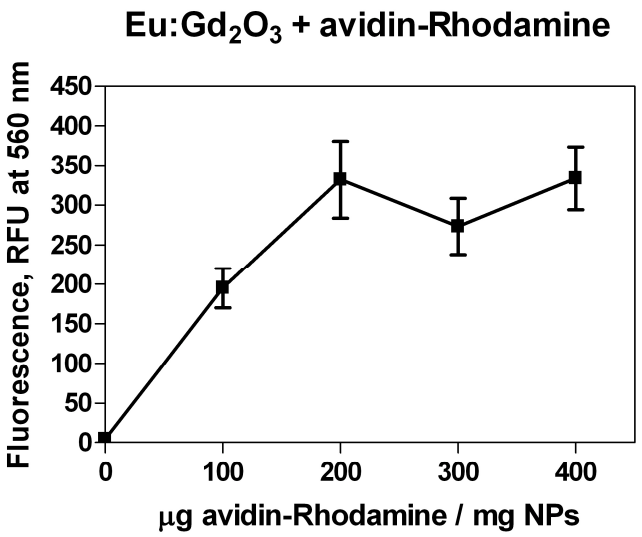

Figure 4. Fluorescence intensity of avidin-rhodamine adsorbed on 1 mg Eu:Gd_2O_3 nanoparticles, measured for different coating concentrations of avidin-rhodamine.

For evaluation of the avidin coating, Eu:Gd_2O_3 particles were coated with rhodamine labeled avidin following the procedure described in the experimental section. The measured fluorescence intensity of rhodamine for different coating amounts of avidin-rhodamine is presented in Fig. 4. For concentrations up to 200 μg ml^{-1}, the fluorescence intensity increased proportionally to the coating amount. This shows that such avidin amounts were not enough to form dense avidin monolayers on the particles surfaces. For concentrations higher than 200 μg ml^{-1}, the rhodamine intensity did not depend on the coating concentration, indicating saturation of the particles surfaces with avidin and the formation of a monolayer. Based on these results, we chose 200 μg avidin per 1 mg nanoparticles as coating concentrations for further experiments.

3.3. Fluorescence imaging of BSA-Biotin micropatterns with avidin - Eu:Gd_2O_3 nanoparticles

The preparation of the BSA-Biotin micropatterns and their interaction with the avidin coated Eu:Gd_2O_3 nanoparticles is schematically presented in Fig. 1 (see Experimental section). The corresponding acquired fluorescent image is shown in Fig. 5. A series of alternating bright strips and dark strips can be observed. The actual width of the strips is 5 μm, which corresponds to the features of the PDMS stamp used for BSA-b printing. The bright strips correspond to the fluorescent Eu:Gd_2O_3 – avidin complexes that were specifically bound to the printed BSA-b. The dark strips, on the other hand, correspond to the BSA - passivated spacings between the printed strips where no avidin coated particles are expected to bind. Although not all the bright strips have perfectly uniform fluorescent intensity, they are covered with specifically bound fluorescent particles without large gaps. Densely packed bound particles show up as higher intensity spots while areas with lower surface density of bound particles are dimmer. On the other hand, very few fluorescent particles can be observed in the BSA – passivated areas, demonstrating very low nonspecific binding in this case. The presence of clearly distinguishable fluorescent strips shows that the specific binding of avidin to biotin was not disturbed by the particles. In addition, the absence of particles between the strips confirms that the blocking of the silicon substrate and the nanoparticles with BSA was sufficient to prevent non-specific binding of nanoparticles onto the substrate.

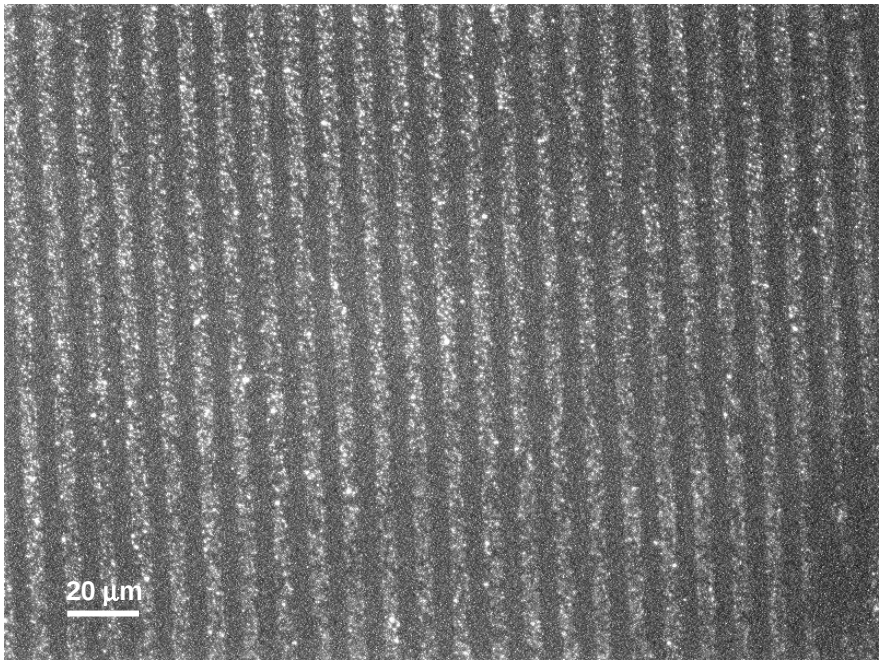

Figure 5. Fluorescent image of specifically immobilized avidin-Eu:Gd_2O_3 nanoparticles on printed BSA-biotin

Another important conclusion is that the non – uniform size distribution of the nanoparticles may not disturb this type of application. This makes possible the use of particles laying into certain size range instead of expensive monodispersed particles. The lack of photobleaching of the Eu:Gd_2O_3 nanoparticles allowed the fluorescent image to be observed for unlimited period of time providing the possibility for image optimization.

3.4. AFM characterization of BSA-Biotin micropatterns with avidin - Eu:Gd_2O_3 nanoparticles

We have employed AFM to image the immobilized avidin-Eu:Gd_2O_3 on a single particle level. The presence of solid nanoparticle labels with sizes larger than those of proteins on the substrate surface makes it possible to evaluate the density of specifically and non-specifically bound particles. AFM topographic image of a randomly chosen region with a scan size of 40x40 μm^2 of the substrate is shown in top part of Fig. 6. Four vertical bright strips are visualized within the scan area as shown in Fig. 6. The discrete nature of the nanoparticles as labels makes that the strips they form look imperfect. The surface density of specifically bound particles on the strips is much higher than the density of non-specifically bound particles shown as scattered bright spots in between the line patterns. The selectivity achieved here is the basis for applying this approach as a detection technique. The observed non-specifically bound particles could be possibly minimized by further optimization of the coating and washing processes. Density of the specifically bound particles can also be improved by optimization of the incubation protocols. In the bottom part of Fig. 6, It is a cursor profile which was taken along the white line in the AFM image. According to the cursor profile, the aggregates on the strips have heights between about 10 and 250 nm. The majority of the aggregates show height between 50 and 100 nm. This height measurement is consistent with the particle size known from TEM studies. It is clear that these aggregates are the immobilized avidin coated nanoparticles.

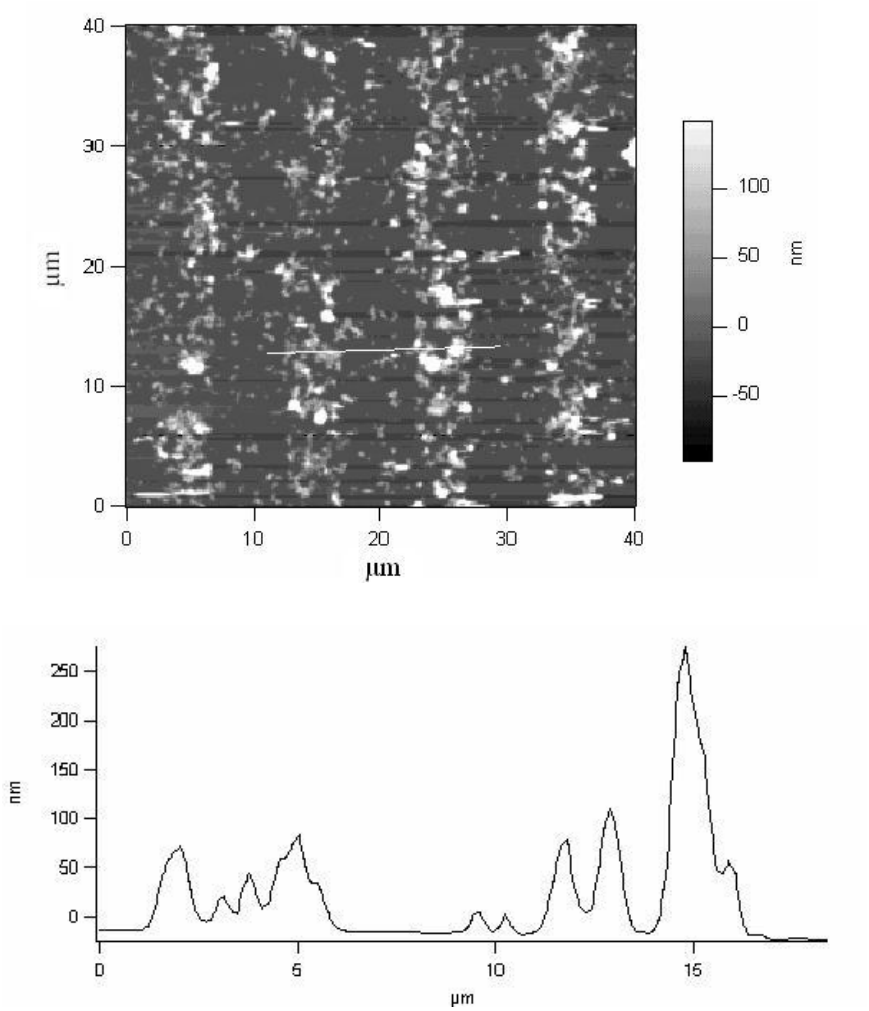

Figure 6. AFM characterization of BSA-Biotin micropatterns with avidin - Eu:Gd_2O_3 nanoparticles. (a) AFM topographic image of a micropatterned BSA-b after incubation with Avidin-Eu particle for 1 h. The image size is 40 x 40 μm^2. (b) The cursor profile along the line in (a) shows that the height of the particles is in the range of 10 to 250 nm.

4. CONCLUSIONS

It is the first time that we demonstrated that the fluorescent nanoparticles made of lanthanide oxides can be successfully used for visualizing protein micropatterns. The unique spectral properties, photostability and low price of synthesis of these novel materials offer an attractive alternative to other widely used fluorophores. The surface properties of the Eu:Gd_2O_3 nanoparticles presented in this paper permit easy one-step bio-functionalization of the particles. The avidin – coating of Eu:Gd_2O_3 nanoparticles can be used as a base-shell for the preparation of nanoparticle conjugates with a variety of biotin-modified antibodies recognizing the desired target, proteins and DNA that are commercially available. Those conjugates could be applied to the fluorescence detection of a variety of molecules in the array format presented here.

Acknowledgments

The authors wish to acknowledge the support of the National Science Foundation, grant DBI-0102662 and the Superfund Basic Research Program with Grant 5P42ES04699 from the National Institute of Environmental Health Sciences, NIH.

REFERENCES

1. R. N. Bhargava, "Doped nanocrystalline materials -- Physics and applications," *Journal of Luminescence*, vol. 70, pp. 85-94, 1996.
2. B. M. Tissue, "Synthesis and luminescence of lanthanide ions in nanoscale insulating hosts," *Chemistry of Materials*, vol. 10, pp. 2837-45, 1998.
3. W. O. Gordon, J. A. Carter, and B. M. Tissue, "Long-lifetime luminescence of lanthanide-doped gadolinium oxide nanoparticles for immunoassays," *Journal of Luminescence*, vol. 108, pp. 339-42, 2004.
4. C. B. Murray, D. J. Norris, and M. G. Bawendi, "Synthesis and Characterization of Nearly Monodisperse Cde (E = S, Se, Te) Semiconductor Nanocrystallites," *Journal of the American Chemical Society*, vol. 115, pp. 8706-15, 1993.
5. J. Feng, G. M. Shan, A. Maquieira, M. E. Koivunen, B. Guo, B. D. Hammock, and I. M. Kennedy, "Functionalized europium oxide nanoparticles used as a fluorescent label in an immunoassay for atrazine," *Analytical Chemistry*, vol. 75, pp. 5282-86, 2003.
6. A. Bernard, E. Delamarche, H. Schmid, B. Michel, H. R. Bosshard, and H. Biebuyck, "Printing patterns of proteins," *Langmuir*, vol. 14, pp. 2225-29, 1998.
7. A. Bernard, J. P. Renault, B. Michel, H. R. Bosshard, and E. Delamarche, "Microcontact printing of proteins," *Advanced Materials*, vol. 12, pp. 1067-70, 2000.
8. Molecular Probes: http://www.probes.com, "Amine-reactive Probes"
9. D. Dosev, B. Guo, and I. M. Kennedy, "Size Effect on Photoluminescence and Crystal Structure of Eu^{3+}:Y_2O_3 Nanoparticles Synthesized by Flame Spray Pyrolysis," submitted for publication to *Journal of Aerosol Science*.
10. R. Tapec, X. J. J. Zhao, and W. H. Tan, "Development of organic dye-doped silica nanoparticles for bioanalysis and biosensors," *Journal of Nanoscience and Nanotechnology*, vol. 2, pp. 405-09, 2002.
11. H. Mattoussi, J. M. Mauro, E. R. Goldman, G. P. Anderson, V. C. Sundar, F. V. Mikulec, and M. G. Bawendi, "Self-assembly of CdSe-ZnS quantum dot bioconjugates using an engineered recombinant protein," *Journal of the American Chemical Society*, vol. 122, pp. 12142-50, 2000.
12. E. R. Goldman, E. D. Balighian, H. Mattoussi, M. K. Kuno, J. M. Mauro, P. T. Tran, and G. P. Anderson, "Avidin: A natural bridge for quantum dot-antibody conjugates," *Journal of the American Chemical Society*, vol. 124, pp. 6378-82, 2002.